The short-term combined effects of temperature and organic matter enrichment on permeable coral reef carbonate sediment metabolism and dissolution

Coulson A. Lantz[1], Kai G. Schulz[1], Laura Stoltenberg[1], Bradley D. Eyre[1]

[1]Centre for Coastal Biogeochemistry, School of Environment, Science, and Engineering, Military Road Southern Cross University Lismore 2480 NSW Australia

Correspondence to: Coulson A. Lantz (Coulsonlantz@gmail.com)

Abstract

Rates of gross primary production (GPP), respiration (R), and net calcification (G_{net}) in coral reef sediments are expected to change in response to global warming (and the consequent increase in sea surface temperature) and coastal eutrophication (and the subsequent increase in the concentration of organic matter (OM) being filtered by permeable coral reef carbonate sediments). To date, no studies have examined the combined effect of seawater warming and OM enrichment on coral reef carbonate sediment metabolism and dissolution. This study used 22-hour *in situ* benthic chamber incubations to examine the combined effect of temperature (T) and OM, in the form of coral mucus and phytodetritus, on GPP, R, and G_{net} in the permeable coral reef carbonate sediments of Heron Island lagoon, Australia. Compared to control incubations, both warming (+2.4 ºC) and OM increased R and GPP. Under warmed conditions, R (Q_{10} = 10.7) was enhanced to a greater extent than GPP (Q_{10} = 7.3), resulting in a shift to net heterotrophy and net dissolution. Under both phytodetritus and coral mucus treatments, GPP was enhanced to a greater extent than R, resulting in a net increase in GPP/R and G_{net}. The combined effect of warming and OM enhanced R and GPP, but the net effect on GPP/R and G_{net} was not significantly different from control incubations. These findings show that a shift to net heterotrophy and dissolution due to short-term increases in seawater warming may be countered by a net increase GPP/R and G_{net} due to short-term increases in nutrient release from OM.

1. Introduction

Despite occupying only 7.5% of the seafloor, coastal marine sediments are responsible for a large fraction (55%) of global sediment organic matter oxidation (Middelburg et al., 1997). Of the coastal marine sediment environments, coral reef sediments are one of the most severely threatened by global climate change (Halpern et al., 2007). Rates of sediment autotrophic production (gross primary productivity; GPP) on coral reefs are generally greater than rates of heterotrophic metabolism (respiration; R) (GPP/R > 1), such that the sediments are generally a net source of oxygen (Atkinson, 2011). Similarly, rates of sediment calcification/precipitation are generally greater than rates of sediment dissolution (G_{net} > 0) on most reefs under current ocean conditions, such that coral reef sediments on 24-hour diel timescales are net precipitating, resulting in the long-term burial of carbon in the form of calcium carbonate (Eyre et al., 2014; Andersson, 2015). This long-term production of calcium carbonate is an important component of reef formation and the creation of sandy cays (Atkinson, 2011). However, due to anthropogenically-mediated processes such as sea surface temperature (SST) warming (Levitus et al., 2000) and coastal eutrophication (Fabricius, 2005), coral reef sediments may soon be subjected to

elevated SSTs and excess loadings of OM (Rabouille et al., 2001). This could ultimately impact the balance in GPP/R and G_{net} in the sediment and potentially alter the long-term accumulation of carbonate material on coral reefs (Orlando and Yee, 2016).

Given the recent projections of SST increases on coral reefs of between 1.2 to 3.2 ºC by the end of this century (IPCC, 2013), there are concerns that the net metabolic balance in coral reef sediments may shift away from net production and net calcification to a state of net heterotrophy and net dissolution (Pandolfi et al., 2011). While several coral reef studies have examined the response in individual calcifying organisms to increased seawater temperature (T) (e.g., Johnson and Carpenter, 2012; Shaw et al., 2016), only one study (Trnovsky et al., 2016) has examined the response in entire permeable coral reef carbonate sediments. Furthermore, the majority of warming studies on marine sediments have been performed *ex situ* in more pole-ward latitudes (temperate to arctic environments) over a wide range of temperatures (2 – 30 ºC) (e.g., Tait and Schiel, 2013; Hancke et al., 2014; Ashton et al., 2017). The bacterial communities residing in marine sediments generally display a hyperbolic temperature-production relationship where GPP increases with T (~ + 32 % per 1 ºC increase) until an optimal rate is reached roughly +2 – 3 ºC above naturally observed seasonal maxima. This T-GPP relationship then declines at higher temperatures (+4 - 6 ºC) due to the deactivation of component reactions (Bernacchi et al., 2001). In Arctic and temperate marine sediment communities, the increase in T can alter the balance between GPP and R, with an observed shift towards net heterotrophy (GPP/R < 1) (e.g., Arnosti et al., 1998; Hancke and Glud, 2004; Weston and Joye, 2005). Trnovsky et al. (2016) found that warming also decreased GPP/R in coral reef sediments and reduced G_{net} due to enhanced sediment dissolution.

Ultimately, the magnitude of potential shifts in coral reef sediment GPP/R and G_{net} under global warming scenarios will depend critically on the availability of organic matter (OM) substrate for remineralisation (Ferguson et al., 2003; Rabalais et al., 2009). Carbonate sediment dissolution is strongly controlled by the extent of OM decomposition in the sediments (Andersson, 2015). Coral reefs are classically characterized as oligotrophic, i.e. relatively deficient in major inorganic nutrients (Koop et al., 2001). Despite this classification, the relatively high rates of GPP (1 to 3 mol C m^{-2} d^{-1}) for these ecosystems (Odum and Odum, 1955) are evidence of a tightly coupled nutrient cycling between autotrophs and heterotrophs. However, the balance in sediment metabolism on coral reefs may change in response to OM over-enrichment associated with eutrophication (Bell, 1992). Coral reefs affected by eutrophication (e.g., Hawaii (Grigg, 1995), Indonesia (Edinger et al., 1998), Jamaica (Mallela and Perry, 2007), Puerto Rico (Diaz-Ortega and Hernandez-Delgado, 2014)) all exhibit elevated concentrations of OM in the water column (particulate OM: 10 – 50 µmol C L^{-1}) and

above average rates of sedimentation (5 – 30 mg cm^{-2} d^{-1}). Elevated concentrations of OM and increased rates of terrestrially derived sedimentation on coral reefs can cause a decline in hard coral cover and a relative increase in macroalgal cover, resulting in an overall degradation of coral reef habitat (Fabricius, 2005).

The amount of OM processed in coral reef sediments can be increased through several processes, two of which were simulated in this study; 1) through local phytoplankton blooms in the water column in response to the runoff of inorganic and organic nutrients and the eventual sediment deposition of dead phytoplankton, referred to herein as phytodetritus (Furnas et al., 2005) and 2) the release of coral mucus into the reef water column as a stress response of scleractinian corals to increased sedimentation and the subsequent sediment deposition of this bacteria-rich protein matrix (Ducklow and Mitchell, 1979). The sediment deposition of OM provides labile carbon substrate (and associated nitrogen and phosphorous) for immediate consumption by autotrophic and heterotrophic bacterial communities.

Studies which have examined the effect of increased concentrations of OM, such as coral mucus (e.g., Wild et al., 2004a [24 hours]) or coral spawn and phytodetritus (e.g., Eyre et al., 2008 [1 week]), on coral reef sediment metabolism have shown a short-term increase in GPP/R, contrasting the results provided from short-term temperature studies on coral reef sediments, where GPP/R decreased (Trnovsky et al., 2016 [24 hours]). Experimental additions of coral mucus from *Acropora* spp. on Heron Island, Australia (conducted only in the dark over 12 hours) induced a ~ 1.5-fold increase in R (Wild et al., 2004b) while additions of *Fungia* spp. mucus from a reef in Aqaba, Jordan (also conducted over 12 hours in the dark; Wild et al., 2005) showed a ~ 1.9-fold increase in R. OM associated with a mass coral spawning event (coral gametes and subsequent phytodetritus produced in the water column) on Heron Island, Australia caused a 2.5-fold increase in sediment R and a 4-fold increase in sediment GPP over the course of a week (Glud et al., 2008). Unlike the short-term response in GPP/R to T, sediment metabolism remained net-autotrophic during the spawning event at Heron Island, with GPP/R ratios rising as high as 2.5 – 3.0 (Glud et al., 2008), implying that nutrients recycled from OM stimulated GPP in excess of R (Eyre et al., 2008) on relatively short timescales (hours to days). However, studies which have examined the effect of excess OM on coral reef sediment metabolism over longer time scales (months) have shown that, ultimately, GPP/R eventually shifts to net heterotrophy (e.g., Andersson, 2015; Yeakel et al., 2015; Muehllehner et al., 2016). This suggests that despite an initial OM-induced increase in GPP/R, the net long-term effect within reef sediments may be a preferentially heterotrophic recycling of nutrients released from organic matter degradation. Altogether, questions remain if a predicted temperature-driven shift to net heterotrophy will be exacerbated or mitigated by the presence of excess organic matter

97 filtered by coral reef sediments. There are, to date, no studies that have examined the effect of OM on coral reef
98 sediment G_{net}. The observed short-term (24 hours to a week) increase in GPP/R in response to OM would imply
99 that sediment G_{net} may also increase given that coral reef sediments generally exhibits a positive GPP/R-G_{net}
100 relationship (Cyronak et al., 2016), whereas the observed long-term (months) decrease in GPP/R may also
101 reduce sediment G_{net}.

102 Therefore, seawater warming and OM enrichment will likely increase GPP and R in coral reef sediments, but,
103 altogether, there is a lack of research on how these perturbations, specifically in combination, will affect the
104 balance in coral reef sediment organic (GPP/R) and inorganic (G_{net}) metabolism. To meet these needs, this study
105 performed incubations using benthic chambers placed *in situ* in a shallow coral reef sediment environment for a
106 period of 24 hours. Phytodetritus and coral mucus were added to chamber seawater under ambient and increased
107 SST (+2.4 ºC) conditions and the corresponding changes in GPP, R, and G_{net} were measured. We hypothesized
108 that the short-term combined treatments of seawater warming and OM loading would enhance GPP and R in the
109 sediment, but, given the previously shown short-term response in GPP/R and G_{net} to seawater warming
110 (decrease in GPP/R and G_{net}) and net response to OM enrichment (decrease in GPP/R, G_{net} response unknown),
111 there would be a net decrease in GPP/R and G_{net} relative to control treatments.

112 **2. Methods**

113 **2.1 Study site**

114 This study was conducted at Heron Island, Australia (23º 27'S, 151º 55'E) in November 2016. The island is
115 situated near the Tropic of Capricorn, at the southern end of the Great Barrier Reef (GBR) and contains a ~ 9 ha
116 island surrounded by a ~ 24 ha coral reef with an average hard coral cover of ~39% (Salmond et al. 2015). The
117 study site was located on the leeward side of the reef flat, roughly 100 m from the island shore, in a sandy patch
118 where water depth varies between ~ 0.1 – 2.7 m due to semi-diurnal tidal changes. The site was predominately
119 covered in permeable $CaCO_3$ sediments (~ 63%) with interspersed patches of hard coral dominated by *Acropora*
120 spp. (Roelfsema et al., 2002). The $CaCO_3$ sediment at this site has a ~ 2:1 ratio of aragonite: high magnesium
121 calcite (Cyronak et al., 2013a). Sediment grain size at this site showed the following relative abundances at each
122 listed size class (Cyronak et al., 2013b): 12.1%. >2 mm, 30.5% between 1 and 2 mm, 27.3% between 500 µm
123 and 1 mm, 14.1% between 250 µm and 500 µm, 11.2% between 125 µm and 250 µm, 4.2% between 63 µm and
124 125 µm, and 0.6%, < 63 µm. For a more detailed overview of the sediment grain characteristics at this site, we
125 direct the reader to Glud et al. (2008) and Cyronak et al. (2013a; 2013b).

126 **2.2 Experimental design**

127 A total of four 22-hour diel incubations were conducted during 5 - 12 Nov 2016 in advective benthic chambers.
128 Benthic net primary production (NPP), gross primary productivity (GPP), respiration (R), and net calcification
129 (G_{net}) were compared under ambient (~ 0.63 µmol C L^{-1}) and elevated concentrations of particulate organic
130 matter (OM) (additions of ~ 21.3 µmol C L^{-1} phytodetritus or ~ 23.6 µmol C L^{-1} coral mucus) at ~ 28.2 ºC and
131 ~ 30.6 ºC in an orthogonal design. Eight chambers were used per incubation day, with each of the four OM-
132 temperature combinations replicated in two randomly assigned chambers (Fig. 1). The first two incubations
133 included two replicate chambers using phytodetritus crossed with temperature (6 and 7 Nov 2016) while the
134 next two incubations included two replicate chambers using coral mucus crossed with temperature (9 and 11
135 Nov 2016). Incubations were started at sunset (18:00) and ended the following day at dusk (16:00). This allowed
136 for a two-hour period (16:00 – 18:00) where chambers could be moved to a new area of sediment, closed, and
137 heated to the desired temperature offset before beginning the next set of incubations.

138 **2.3 Benthic chambers**

139 Advective benthic chambers were constructed out of clear acrylic with a height of 33 cm and a diameter of 19
140 cm (Huettel and Gust, 1992). A motorized clear disc in the top of the chamber was programmed to spin at a rate
141 of 40 revolutions per minute, which had previously been determined to induce an advection rate of ~ 43 L m^{-2} d^{-1}
142 at the study site (Glud et al., 2008). About 10 - 12 cm of the base of the chamber was inserted into the
143 sediment such that a ~ 4 L water column of seawater was enclosed within the chamber (height ~ 15 cm) upon
144 closing by the lid. The exact water volume varied within each chamber and was calculated for each incubation
145 by multiplying known areal coverage by measured chamber height (at three positions above the sediment). Prior
146 to closing the chambers, the tops were left open for ~ 1 hour to allow settlement of disturbed sediment.
147 Chambers were then sealed ~ 1 hour prior to the beginning of each incubation to allow each temperature
148 treatment chamber to reach the desired temperature offset. Following this, at the beginning of each incubation,
149 selected chambers (four of the eight) were injected with OM (either coral mucus or phytodetritus).

150 **2.4 Temperature manipulation**

151 The international panel on climate change (IPCC) representative concentration pathway (RCP) 8.5 projects an
152 average 2.2 - 2.7 ºC increase in SST (IPCC, 2013). A similar increase in temperature within the benthic
153 chambers was achieved with 5W, silicone-heating pads (RS Australia) inserted inside of each of the four
154 temperature treatment chambers (e.g., Trnovsky et al., 2016). These pads resided in the middle of the chamber

155 water column and were powered by a 12 V battery on a surface support station tethered roughly 3 m away.
156 Temperature and light was measured in all eight chambers and in the water column using HOBO temperature
157 loggers, which recorded temperature (ºC) and light (Lux) at an interval of fifteen minutes. Light intensity (Lux)
158 was converted to µmol quanta of photosynthetic active radiation (PAR) m^{-2} s^{-1} using a conversion factor of
159 0.0185, derived from correlations with PAR measurements of a calibrated ECO-PAR (Wetlabs) sensor over a
160 period of five days ($R^2 = 0.89$).

161 Heating pads increased temperature (T) within the chambers by 2.4 ± 0.5 ºC and maintained this offset on top of
162 the natural diel temperature fluctuations measured in the control chambers (Table 1). As HOBO temperature
163 loggers may record potentially higher than surrounding seawater temperatures due to internal heating of the
164 transparent plastic casing (Bahr et al., 2016; Trnovsky et al., 2016), HOBO temperature data was corrected for
165 precision (48-hour side-by-side logging of all nine loggers in an aquarium) and accuracy (deployment next to an
166 *in situ* SeapHOx (Sea-Bird Electronics) for 48 hours). The conductivity sensor of the SeapHOx was used to
167 record water column salinity for the duration of the experiment (7 days) at a sampling frequency of 30 minutes.

168 **2.5 Organic matter manipulations**

169 Phytodetritus (PD) was injected into treatment chambers to achieve a concentration increase by ~ 20 µmol C L^{-1}
170 , a value analogous to mean conditions observed on degraded eutrophic coral reefs, where water column
171 concentrations can range from 10 to 50 µmol C L^{-1} (Fabricius et al., 2005, Diaz-Ortega and Hernandez-Delgado,
172 2014). Phytodetritus was produced from unfiltered seawater (6 L) collected from the coastal ocean adjacent to
173 the SCU laboratories (Lennox Head, NSW, Australia) and containing naturally occurring assemblages of
174 phytoplankton species common to the East Australian current. Phytoplankton growth in the collected seawater
175 was stimulated by additions of 128 µmol L^{-1} NO_3^-, 8 µmol L^{-1} $PO_4^{3-,}$ and 128 µmol L^{-1} H_4SiO_4 (buffered by
176 additions of 256 µmol L^{-1} of HCl), and a solution of trace metals and vitamins ($F_{1/8}$; Guillard, 1975). Total
177 amounts of nutrients were chosen to allow for a community production of up to 850 µmol C L^{-1} assuming a
178 classical C: N: P Redfield ratio of 116:16:1 and a N:Si requirement of diatoms of 1. After a week of incubation
179 at 150 µmol quanta of PAR m^{-2} s^{-1} at 20 ºC, the phytoplankton community was concentrated to $1/50^{th}$ the
180 original volume (0.12 L) via gentle (> -0.2 bar) vacuum filtration over GF/F filters and rinsed with artificial
181 seawater to remove residual concentrations of dissolved organic and inorganic nutrients. The resulting
182 phytoplankton concentrate (measured at 8.5 mmol C mL^{-1} and 0.9 mmol N mL^{-1} of particulate organic carbon
183 (POC) and nitrogen (PON), respectively, see section 2.6 for details) was stored in the dark at 4.0 ºC until

184 experimental use (6 days). At the beginning of an incubation, 10 ml of the dead phytoplankton concentrate,
185 referred to as PD hereafter, was injected into each treatment chamber (~4 L volume), raising the concentration
186 of carbon and nitrogen by ~ 21.3 ± 1.0 µmol C L^{-1} and ~ 2.2 ± 0.8 µmol N L^{-1}, respectively (Table 1).

187 The amount of coral mucus (CM) added to the chambers was chosen to represent a reef-wide discharge based on
188 reported average mucus secretion rates for *Acropora* spp. (4.8 L mucus m^{-2} d^{-1}; Wild et al., 2004a), the dominant
189 genus on the Heron Island reef flat. Mucus was collected from scattered branching coral fragments (*Acropora*
190 spp.) using a non-destructive method whereby loose individual colonies naturally exposed to air during low tide
191 were inverted so that gravity facilitated the pooling of secreted mucus through a cone filter into a large, 5 L
192 beaker. This mucus was returned to the lab, particle filtered (5.0 µM) to remove the bulk of seawater, re-filtered
193 to separate out particle carbonates, and stored in the dark at 4.0 ºC until experimental use (2 days). Ninety-four
194 ml of mucus was injected into each treatment chamber to simulate the equivalent reported *Acropora* spp. mucus
195 secretion rate (4.8 L mucus m^{-2} d^{-1}) for Heron Island given the average percent of this secreted mucus filtered by
196 the sand (~ 70%; Wild et al., 2004a) and the benthic area enclosed by each chamber (0.028 m^2). Based on
197 measured POC and PON concentrations of the mucus (1.2. mmol C mL^{-1} and 0.08 mmol N mL^{-1}, respectively;
198 see section 2.6) this represented an addition of ~ 23.6 ± 1.1 µmol C L^{-1} and 1.4 ± 0.4 µmol N L^{-1} (Table 1).

199 **2.6 Sample collection and analysis**

200 Seawater samples (120 ml total) were extracted from the top of each chamber via two two-port valves using two
201 60 ml syringes without headspace at ~12 hour intervals (sunset, dawn, and dusk) and returned to the lab for
202 immediate analysis and/or preservation. 10 ml of unfiltered seawater from each chamber was analysed for
203 dissolved oxygen (DO; mg L^{-1}) with a Hach HQ 30d meter and Luminescent DO (LDO) probe. Samples for
204 seawater total alkalinity (A_T; µmol kg^{-1}) were filtered (0.45 µm; Chanson and Millero, 2007) and stored in 100
205 ml plastic, airtight bottles for immediate analysis (< 24 hours). Samples for dissolved inorganic carbon (DIC;
206 µmol kg^{-1}) were also filtered (0.45 µM) into the bottom of 6 ml vials with 5 ml overflow, poisoned (6 µl of
207 saturated $HgCl_2$; Dickson, 2007) and crimped (rubber butyl septum).

208 Seawater A_T was analysed using a potentiometric titration method (Dickson, 2007) on a Metrohm 888 Titrando
209 automatic titrator using ~ 10 ml of weighed-in seawater per sample. DIC was analysed in triplicates on a
210 Marianda AIRICA coupled to a Li-COR LI 7000 CO_2/H_2O Analyzer on 0.4 ml of seawater per sample. A_T and
211 DIC sample precision was estimated with replicate analyses conducted on every fifth sample (A_T SD = ± 1.7
212 µmol kg^{-1}; DIC SD = ± 1.8 µmol kg^{-1}). Measurements were corrected against certified reference material (CRM;

Batch 155) from the Scripps Institute of Oceanography (A_T SD = ± 2.2 µmol kg^{-1}; DIC SD = ± 1.3 µmol kg^{-1}). Parameters for the seawater carbonate system (Ω_{ar}, pH_T (total scale)) were calculated from measured A_T, DIC, temperature, and salinity using the R package seacarb (Lavigne and Gattuso, 2013) with K_1 and K_2 constants applied from Mehrbach et al. (1973) and refit by Dickson and Millero (1987) and the total borate to salinity relationship adapted from Lee and Millero (1995). Because changes in A_T could be due to processes other than the precipitation and dissolution of carbonates (e.g., sulfate reduction associated with organic matter additions), fluxes in DIC were corrected for assumed A_T fluxes due to calcium carbonate precipitation/dissolution (0.5 moles CO_2: 1 mole A_T) and compared against fluxes in O_2, with an expected 1:1 molar flux ratio (DIC_{org} : O_2).

Prior to chamber additions subsamples (1 ml, n = 3) were taken from the concentrated PD culture, CM, and the water column and analysed for particulate organic carbon (POC) and nitrogen (PON). These subsamples were filtered on pre-combusted 25mm GF/F filters, dried at 60 ºC, fumed with 12 M HCl to dissolve any particulate carbonates on the filter, and wrapped in pre-combusted tin capsules. These capsules were analysed for carbon (C) and nitrogen (N) using an elemental analyser (Thermo Flash ES) coupled to an isotope ratio mass spectrometer (Thermo Delta V PLUS) via a Thermo Conflo V (see Eyre et al. 2016, for details).

2.7 Calculating sediment metabolism

Benthic metabolism (NPP, GPP, R, G_{net}) in each chamber was estimated based on the fluxes of measured solutes (DO, and A_T, respectively). For flux calculations, DO was converted from mg L^{-1} to mmol L^{-1}. A_T and DIC were converted from µmol kg^{-1} to mmol L^{-1} using calculated temperature and salinity dependent seawater density. The solute flux equation (Glud et al., 2008) was as follows:

$$Equation 1: F = \frac{\Delta S \times v}{A \times \Delta t}$$

Where F (mmol m^{-2} hr^{-1}) is the net flux in solute, ΔS (mmol L^{-1}) is the change in solute concentration, v (L) is the chamber volume, A (m^2) is the area of sediment enclosed by the chamber, and Δt (hours) is the time elapsed between seawater samplings. Rates of sediment net primary production (NPP), gross primary production (GPP), and respiration (R) were calculated from O_2 fluxes (mmol O_2 m^{-2} hr^{-1}), and rates of net sediment calcification (G_{net}) were calculated from A_T fluxes (mmol $CaCO_3$ m^{-2} hr^{-1}) (Table 2). Both NPP and GPP are reported as positive values to represent flux of O_2 from the sediment into the chamber water column whereas R is reported as a negative value to represent the flux of O_2 from chamber water column into the sediment. To calculate the ratio of GPP/R, positive values of R were used. To determine the sensitivity of GPP and R to changes in

241 temperature, the absolute difference in diel GPP and R (mmol O_2 m^{-2} d^{-1}) between the control and warming
242 treatments was divided by the increase in temperature (2.4 ± 0.5 ºC) to provide a mmol O_2 m^{-2} d^{-1} $ºC^{-1}$ sensitivity
243 metric. Additionally, to provide comparability with the literature and determine the numerical relationship
244 between a 10 ºC change in temperature and GPP and R, Q_{10} values were estimated for temperature treatments
245 according to the following equation:

$$Equation2: Q_{10} = \left(\frac{M2}{M1}\right)^{\left(\frac{10}{T_2 - T_1}\right)}$$

246 where *M1* is the metabolic rate (GPP or R) at temperature T_1 (control) and *M2* is the metabolic rate (GPP or R,
247 respectively) at temperature T_2 (warming treatment), with $T_1 < T_2$.

248

249 **2.8 Statistical analyses**

250 Results are displayed as the mean ± standard deviation (SD). Data were organized as the hourly average for both
251 day and night and were pooled together within each T, OM, and T + OM treatment where results did not
252 significantly differ between incubations. All statistical analyses were performed with the SPSS statistics
253 software (SPSS Inc. Version 22.0) running in a Windows PC environment, and the assumptions of normality
254 and equality of variance were evaluated with graphical analyses of the residuals. To test for the effect of each
255 treatment (T, PD, and CM) on respiration, photosynthesis, and calcification, measured R, NPP, GPP, and G_{net}
256 were analysed using a repeated-measures three-way analysis of variance (ANOVA). In this model, temperature
257 and OM (PD and CM) were fixed effects, the within-subject factor was time (days), and replicate chambers
258 were a nested effect. To compare the significance of temperature and OM between and within treatment
259 chambers, a one-way ANOVA model was used in which chamber was the fixed effect and average seawater
260 temperatures (ºC) and POC and PON concentrations, respectively, were treated as the response variable. In these
261 analyses, Bonferroni post-hoc test were used to conduct pair-wise comparisons between treatments.

262 **3. Results**

263 **3.1 Measured seawater chemistry and sediment metabolism in control chambers**

264 Temperatures measured in both the water column and chambers exhibited typical diel changes, and were
265 slightly warmer in the controls (28.2 ± 1.3 ºC) in comparison to the water column (-0.8 ± 0.5 ºC) (Fig. 2). Mean
266 water column salinity throughout the experiment was 35.8 ± 0.1. Over the course of each diel incubation period,

changes in water chemistry (Fig. 3) were driven by benthic metabolism. Control (C) chambers, over the diel cycle, were net autotrophic and net calcifying. C chambers were net dissolving at night and net calcifying during the day. Mean particulate organic carbon (POC) and nitrogen (PON) concentrations in the four C chambers were 0.63 ± 0.1 µmol C L^{-1} and 0.12 ± 0.1 µmol N L^{-1}, respectively. The DIC_{org}:O_2 quotient for all treatments was 0.94 ± 0.09 on average and did not significantly differ from 1 ($p < 0.05$; Fig. 4), suggesting that sulphate reduction did not significantly contribute to the A_T fluxes.

3.2 The effects of temperature on sediment metabolism

Mean seawater temperature in the C and temperature (T) treatments during the four incubation periods was 28.2 ± 1.1 ºC and 30.6 ± 1.2 ºC, respectively (Table 1). Temperature differed between C and T treatments ($F_{1,31}$ = 384.38, $p < 0.05$), but there was no significant difference between replicate chambers within each treatment ($F_{1,31}$ =0.76, $p = 0.768$). Temperature in all eight chambers exhibited typical diel changes throughout all four incubation periods, driven by sunlight and tidal changes in water depth (Fig. 2). Treatment chambers followed the same natural diel change measured in control chambers and maintained an average + 2.4 ± 0.5 ºC offset over the course of the study (Table 1).

During the fourth set of incubations, one T treatment was lost due to a broken heater and this chamber was treated as a third control. Seawater warming increased R ($F_{1,31}$ = 260.38, $p < 0.05$), NPP ($F_{1,31}$ = 192.17, $p < 0.05$), and GPP ($F_{1,31}$ = 160.61, $p < 0.05$) (Table 3, Fig. 5). Overall, warming decreased GPP/R ($F_{1,31}$ = 79.02, $p < 0.05$) from a state of net autotrophy to net heterotrophy (Fig. 6). Mean calculated temperature sensitivity, averaged across T treatments from all four incubations, was 22.3 ± 3.8 mmol O_2 m^{-2} d^{-1} ºC^{-1} for R and 16.1 ± 2.8 mmol O_2 m^{-2} d^{-1} ºC^{-1} for GPP. Mean calculated Q_{10} values were 10.7 ± 3.1 for R and 7.3 ± 1.2 for GPP. Warmed chambers were net dissolving at night and net calcifying during the day. Overall, warming caused a net decrease in diel G_{net} ($F_{1,31}$ = 122.82, $p < 0.05$) from a state of net calcification to net dissolution (Fig. 7).

3.3 The effects of organic matter on sediment metabolism

Mean POC and PON concentrations in the four phytodetritus (PD) treatment chambers were 21.7 ± 1.0 µmol C $L^{-1}$and 2.3 ± 0.8 µmol N L^{-1}, respectively (POC:PON ~ 9:1) (Table 1). PD increased R ($F_{1,15}$ = 16.77, $p < 0.05$), NPP ($F_{1,15}$ = 245.86, $p < 0.05$), and GPP ($F_{1,15}$ = 212.64, $p < 0.05$). Overall, PD caused a net increase in GPP/R

294 ($F_{1,15}$ = 13.92, $p < 0.05$) (Table 3). Chambers treated with PD were net dissolving at night and net calcifying
295 during the day. Overall, PD caused a net increase in diel G_{net} ($F_{1,15}$ = 134.27, $p < 0.001$).

296 Mean POC and PON concentrations in the four coral mucus (CM) treatment chambers were 24.2 ± 1.1 µmol C
297 L^{-1} and 1.5 ± 0.4 µmol N L^{-1}, respectively (POC:PON ratio ~ 16:1). CM increased R ($F_{1,15}$ = 7.34, $p < 0.05$),
298 NPP ($F_{1,15}$ = 134.51, $p < 0.05$), and GPP ($F_{1,15}$ = 99.24, $p < 0.05$). Overall, CM caused a net increase in GPP/R
299 ($F_{1,15}$ = 34.17, $p < 0.05$) (Table 3). Chambers treated with CM were net dissolving at night and net calcifying
300 during the day. Overall, CM caused a net increase in diel G_{net} ($F_{2,22}$ = 100.61, $p < 0.05$).

301 **3.4 The combined effects of temperature and organic matter on sediment metabolism**

302 In the first two incubations, T + PD increased R ($F_{1,15}$ =46.4 $p < 0.001$), NPP ($F_{1,15}$ =16.31, $p < 0.05$), and GPP
303 ($F_{1,15}$ =8.81, $p < 0.05$) (Table 3). However, GPP/R in T + PD treatments did not significantly differ from control
304 chambers ($F_{1,15}$ =2.75, p = 0.122). Chambers treated with T + PD were net dissolving at night and net calcifying
305 during the day. Overall, diel G_{net} in T + PD treatments did not significantly differ from control chambers ($F_{1,15}$
306 =0.70, p = 0.417).

307 In the two last incubations T + CM and increased R ($F_{1,15}$ =7.75, $p < 0.05$), NPP ($F_{1,15}$ =17.19, $p < 0.05$), and
308 GPP ($F_{1,15}$ =26.77, $p < 0.05$) (Table 3). With 1.21 ± 0.13 GPP/R in the T + CM treatments was again not
309 significantly different from control chambers ($F_{1,15}$ =3.79, p = 0.075). T + CM chambers were net dissolving at
310 night (-1.8 ± 0.3 mmol $CaCO_3$ m^{-2} hr^{-1}) and net calcifying during the day (2.4 ± 0.4 mmol $CaCO_3$ m^{-2} hr^{-1}).
311 Overall, 24-hour diel G_{net} in T + CM treatments was 0.2 ± 0.2 mmol $CaCO_3$ m^{-2} hr^{-1}, a change which was not
312 significantly different from control chambers ($F_{1,15}$ =0.87, p = 0.368).

313 **4. Discussion**

314 **4.1 The response in coral reef sediment metabolism to seawater warming**

315 Under control conditions, rates of GPP, R, and G_{net} were similar to those measured in advective benthic
316 chambers simulating equivalent percolation rates (Table 4) over 24-hour diel timescales. Furthermore,
317 carbonate sediments were net autotrophic (GPP/R = 1.31 ± 0.1), similar to previous studies (Eyre et al., 2014).
318 The sediments were net calcifying during the day under all treatment conditions, which was likely due to a
319 combination of light-stimulated biogenic calcification by infaunal organisms (e.g., symbiont-bearing
320 foraminifera [Yamano et al., 2000] or dinoflagellates [Frommlet et al., 2015]) and by a photosynthetically-
321 mediated increase in porewater aragonite saturation state to a value that would allow for abiotic precipitation (Ω

> 8; [Cohen et al., 2009]). However, the exact organisms and geochemical conditions responsible for the measured net diurnal calcification signal was beyond the scope of this study and should be examined in future work.

It should also be noted that the daytime incubations in this study were terminated at 16:00, 2 hours before of sunset (18:00), to allow time to move each chamber and establish new treatment conditions for the next set of incubations. It is therefore possible that the calculated daytime GPP was slightly overestimated given that the sediments in these final 2 hours before sunset generally exhibit a lower rate of oxygen production relative to the 6:00 to 16:00 time period due to a reduction in light intensity (Cyronak et al., 2013b). However, a comparison of the mean GPP in control chambers to prior chamber work at the same study site, where incubations lasted until sunset (Cyronak et al., 2016; Table 4), shows that GPP in this study was lower. This suggests that temporal variability in light intensity, temperature, and other abiotic factors likely exerts a greater influence on GPP than a 2-hour difference in incubation period.

In our experiments, seawater warming (+2.4 ± 0.5 ºC) was within the projection of the IPCC RCP 8.5 (+2.2 – 2.7 ºC). Under this elevated seawater temperature, R increased to a greater extent than GPP, shifting the sediments to net heterotrophy (GPP/R = 0.93) over the diel incubation period (Fig. 8). The decrease of GPP/R due to warming can be explained by the relatively lower temperature sensitivity value for GPP (16.1 ± 2.8 mmol O_2 m^{-2} d^{-1} ºC^{-1}) compared to R (22.3 ± 3.8 mmol O_2 m^{-2} d^{-1} ºC^{-1}). This is further supported by the relatively lower measured Q_{10} value for GPP (7.3 ± 1.2) compared to R (10.7 ± 3.1), similar to those measured by Trnovsky et al. (2016) for GPP (3.1 – 4.1) and R (7.4 to 13.0). It is important to note that the established Arrhenius relationships in the literature suggest that development and growth rates should increase at a rate of 7 – 12 % per 1 ºC of warming (Clarke, 2003), much lower than the observed 74 % and 42 % increase in R and GPP, respectively, per 1 ºC of warming in this study. However, recent work in the Antarctic by Ashton et al. (2017) on marine benthic assemblages showed that, in some species, the growth rate exhibited a 100% increase per 1 ºC of warming, yielding Q_{10} values around 1,000. Therefore, while the temperature sensitivity estimates reported in this manuscript and in Trnovsky et al. (2016) exceed the expected rate for biological reactions and enzyme activity, evidence exists in other benthic marine environments to support the notion that the impact of temperature on biochemical processes may be more complex than previously thought at the organism level (Ashton et al., 2017).

Overall, the response in GPP/R to temperature agrees with other studies showing that seawater warming preferentially enhances R to a greater degree than GPP in marine sediments (Hancke and Glud, 2004; Weston and Joye, 2005; Tait and Schiel, 2013). The decline in GPP/R in response to warmer seawater temperature may be a product of the differential ranges in activation energies for GPP and R (Yvon-Durocher et al., 2010), where R exhibits a stronger and more rapid physiological acclimation to warming compared to GPP during short-term temperature variations (Wiencke et al., 1993; Robinson, 2000). The observed 29% decrease in GPP/R in response to warming lead to a net 109% decrease in G_{net} (relative to control chambers), resulting in a transition to net sediment dissolution over the diel incubation period (Fig. 8). This decrease in G_{net} was most likely due to a respiration-driven increase in porewater pCO_2 (e.g., Cyronak et al., 2013a), thereby decreasing pH and the mean porewater aragonite saturation state, as evidenced by decreasing water column levels (mean Ω_{arg} = -0.7 relative to control chambers). While rising T increases Ω_{arg} geochemically, with less than 0.03 units per degree of temperature increase, this effect is negligible and by far outweighed by biologically driven changes in Ω_{arg}, leading to an overall decrease. In summary, a warming of seawater by 2.4 ºC decreased GPP/R by 0.38 units and G_{net} by 0.2 mmol $CaCO_3$ m^{-2} hr^{-1} in the permeable calcium carbonate sediments at this study site on Heron Island. The decline in the GPP/R in response to warming implies that a greater fraction of the carbon fixed by autotrophs was remineralised by heterotrophic bacteria and released as CO_2, thus compromising the capacity of coral reef permeable carbonate sediments to remain net autotrophic at an elevated seawater T.

While a decline in marine sediment GPP/R in response to seawater warming has been previously reported in several studies (e.g., Woodwell et al., 1998; Hancke and Glud, 2004; Weston and Joye, 2005; Lopez-Urrutia and Moran, 2007), the response in G_{net} has only been examined by Trnovsky et al. (2016). It is important to note that these results should not be extrapolated beyond 2100, where SST rises above +2.4 ºC. The T increase simulated in this study (+2.4 ºC) was within the optimal temperature range (30.6 ºC) of previously reported temperature-metabolism hyperbolic relationships in marine sediments (Yvon-Durocher et al., 2010). Given the nature of hyperbolic relationships a further increase in temperature will eventually have an opposite effect on sediment metabolism (net decrease in GPP and R; Weston and Joye, 2005). Thus, the temperature sensitivity reported here should not be extrapolated beyond 2.4 degrees Celsius.

4.2 The response in coral reef sediment metabolism to organic matter enrichment

Increased concentrations of organic matter (OM), analogous to eutrophic conditions on degraded coral reefs, enhanced both GPP and R in the sediment, likely by releasing nitrogen and phosphorus via organic matter

379 degradation. These results agree with prior work, where increased concentrations of OM were quickly
380 aerobically degraded by bacteria within minutes (Maher et al., 2013) to hours (Ferrier-Pages et al., 2000) and
381 enhanced GPP more than R (Glud et al., 2008; Eyre et al., 2008). While some of this OM was likely degraded in
382 the water column, previous experiments (e.g., Wild et al., 2004b) have shown that the high permeability of
383 carbonate sediments permits the transport of OM into the upper centimetres (1 - 4 cm) of the sand, where
384 bacterial degradation rates can exceed those of the water column by a factor of 10-12 (Moriarty, 1985;
385 Wilkinson, 1987).

386 Phytodetritus (PD) and coral mucus (CM) enhanced respiration rates 1.1- and 0.6-fold, respectively, which was
387 a less pronounced increase in R than the 1.5-fold increase observed by Wild et al. (2004b) using the same
388 *Acropora* spp. mucus at Heron Island. This difference may be due to the fact their study used almost three times
389 more CM (~ 280 ml) per treatment than this study (94 ml). An increase in GPP/R to 1.7 one day following the
390 deposition of coral spawning material at the same study site (Glud et al., 2008), was similar to the average
391 increase in GPP/R to 1.6 observed under increased OM concentrations in this study. PD enhanced GPP and R to
392 a greater degree than CM, which may be explained by the higher nitrogen content, or more precisely, the lower
393 C/N ratio in the former. Particulate organic carbon additions differed by less than 10% between PD and CM
394 treatments, whereas particulate organic nitrogen addition (N) was almost twice as high by PD compared CM. In
395 general, bacterial communities responsible for the cycling of nutrients in sediments are thought to be nitrogen
396 limited (Eyre et al., 2013). Given the relatively short timescale (24 hours) in which the response in sediment
397 metabolism to OM was measured, we reason that the PD was more rapidly mineralized than CM due to a higher
398 N content in the added PD (Oakes et al., 2011).

399 To our knowledge, this is the first experiment to examine the short-term relationship between OM degradation
400 and G_{net} in coral reef sediments. Our results show that increased concentrations of PD and CM both enhanced
401 G_{net}. Most likely the increase in G_{net} was a product of the same biogeochemical mechanism influencing G_{net}
402 under seawater warming, whereby changes in GPP/R modify porewater pCO_2 and thus Ω_{arg}. In the case of OM,
403 a preferential enhancement of GPP over R resulted in an increase in Ω_{arg} (mean Ω_{arg} = +0.6 relative to control
404 chambers) and subsequent increase in G_{net} (+1.4 mmol $CaCO_3$ m^{-2} hr^{-1} relative to control chambers). While the
405 results presented here are the first to report a positive OM-G_{net} relationship specifically in permeable calcium
406 carbonate sediments, a similar response has also been observed at ecosystem level in coral reefs (Yeakel et al.,
407 2015), where increased offshore productivity in the Sargasso Sea over the course of several months lead to an
408 increase in community G_{net} on the adjacent Bermuda coral reef flat. Interestingly, this increase in G_{net} in

409 Bermuda coincided with a period of net heterotrophy on the reef. The difference in the G_{net} – GPP/R
410 relationship between the data in this study (OM increased GPP/R and increased G_{net}) and those in Yeakel et al.
411 (2015) (OM decreased GPP/R and increased G_{net}) may be a result of the timescale of observation. This implies
412 that, should elevated concentrations of OM persist for an extended period of time (weeks to months), the
413 immediate preferentially phototrophically-mediated recycling of nutrients, and associated increased GPP/R and
414 G_{net} in coral reef sediments, may eventually shift to net heterotrophy despite the ability to maintain a positive
415 G_{net}.

416 **4.3 The response in coral reef sediment metabolism to a combination of seawater warming and organic**
417 **matter enrichment**

418 The combination of seawater warming and increased concentrations of OM, for both PD and CM, enhanced
419 GPP (+17% relative to the temperature alone) and R (+11% relative to temperature alone) but countered the
420 effect on GPP/R and G_{net} (no significant difference from the control). Given the effect of each of these
421 treatments (T and OM) independently on sediment GPP/R and G_{net}, this result is not surprising. A decrease in
422 GPP/R and G_{net} due to warming was countered by an increase in GPP/R and G_{net} due to an increased
423 concentration of OM.

424 This finding raises questions within the context of each treatment, as mean SST on coral reefs will continuously
425 rise from now until beyond 2100, consistently affecting sediment metabolism. However, organic matter
426 enrichment of permeable coral reef carbonate sediments is also likely to gradually increase due to enhanced
427 algal production from elevated nutrients (Furnas et al., 2005), elevated terrestrial input of OM (Diaz-Ortega and
428 Hernandez-Delgado, 2014) and enhanced mucus production due to enhanced terrestrial sedimentation (Alongi
429 and McKinnon, 2005). As discussed above this long-term enrichment with OM will most likely make coral reef
430 sediments more heterotrophic (and not more autotrophic as in this short-term study). However the subsequent
431 response in G_{net} over longer timescales is less clear, as some work has shown that the degradation of organic
432 matter can enhance sediment dissolution (Andersson, 2015) whereas other work (e.g., Yeakel et al., 2015) has
433 shown that community calcification may actually increase. Therefore, combined with an increase in T, the effect
434 of long-term enrichment of OM on GPP/R is likely to be additive (decrease GPP/R), but the long-term response
435 in G_{net} still needs to further examination.

436 Similarly, the effect of other, more persistent products of eutrophication, namely dissolved inorganic nutrients
437 (DIN: NH_4^+, NO_3^-, PO_4^{3-}), on coral reef sediment GPP/R and G_{net} have yet to be studied and may become more

frequent and persistent as coastal land use changes continue to facilitate the increased runoff of fertilizers (Koop et al., 2001). Consequently, the results presented here provide an estimation of the future short-term response in coral reef sediment GPP/R and G_{net} to warming (+2.4 ºC) and eutrophication (PD and CM), but by no means have explored other potential warming- and eutrophication-mediated perturbations that continue to threaten coral reef ecosystems. Future work should consider varying durations (e.g., > 24 hours) and forms of eutrophication (e.g., DIN) as well as a range of T, both within and beyond reported optimal ranges (> 2.4 ºC), to better constrain our understanding of the potential feedback responses in coral reef sediment GPP/R and G_{net}.

4.4 Conclusions

This study suggests that seawater warming will shift GPP/R and G_{net} in permeable calcium carbonate coral reef sediments to a state of net heterotrophy and net dissolution, respectively, by the year 2100. In contrast, short-term eutrophication, and the subsequent production of OM in the form of phytodetritus and coral mucus, could enhance sediment GPP/R and G_{net}. The combined effect of seawater warming and increased concentrations of OM may additively enhance sediment GPP and R, but the net effect on GPP/R and G_{net} will likely counter one another on relatively short timescales of days. The future response in the net-flux-behaviour of CO_2 and O_2 in the coral reef sediment environment, and the consequent rate of carbon sequestration into the sediments, will likely depend on the relative frequency and duration of each perturbation. The effects of OM (e.g., phytoplankton growth, reef-wide mucus secretion) on sediment metabolism generally persist temporarily (days to weeks) relative to global warming, a constant process which will continue to occur throughout this century and beyond. Provided this ecological context and the findings from this study, we propose that increased concentrations of OM, in the form of phytodetritus and coral mucus, will increase G_{net} and GPP/R in the sediment on relatively short timescales. However, once seawater temperature on coral reefs rises 2.4 ºC above the present day mean, the immediate effect of OM on sediment metabolism will be compromised by a warming-mediated net decrease in G_{net} and GPP/R, thereby limiting the ability of permeable calcium carbonate sediments on coral reefs to accumulate calcium carbonate.

Acknowledgements

We would like to thank Jacob Yeo for his assistance in the field. This research was funded by ARC Discovery Grant DP150102092 and conducted under the GBRMPA permit number G16/38438.1.

References

Alongi, D. M. and McKinnon, A. D.: The cycling and fate of terrestrially-derived sediments and nutrients in the coastal zone of the Great Barrier Reef shelf, in Marine Pollution Bulletin, vol. 51, pp. 239–252, 2005.

Andersson, A. J.: A fundamental paradigm for coral reef carbonate sediment dissolution, Front. Mar. Sci., 2, 52, doi:10.3389/fmars.2015.00052, 2015.

Ashton, G. V., Morley, S. A., Barnes, D. K. A., Clark, M. S. and Peck, L. S.: Warming by 1°C Drives Species and Assemblage Level Responses in Antarctica's Marine Shallows. Current Biology,10.1016/j.cub.2017. 07.048, 2017.

Atkinson, M. J.: Biogeochemistry of nutrients, in Coral Reefs: An Ecosystem in Transition, pp. 199–206, Springer Netherlands, Dordrecht., 2011.

Bahr, K. D., Jokiel, P. L. and Rodgers, K. S.: Influence of solar irradiance on underwater temperature recorded by temperature loggers on coral reefs, Limnol. Oceanogr. Methods, 14(5), n/a-n/a, doi:10.1002/lom3.10093, 2016.

Bell, P. R. F.: Eutrophication and coral reefs-some examples in the Great Barrier Reef lagoon, Water Res., 26(5), 553–568, doi:10.1016/0043-1354(92)90228-V, 1992.

Bernacchi, C. J., Singsaas, E. L., Pimentel, C., Portis, a. R. R. and Long, S. P.: Improved temperature response functions for models of Rubisco-limited photosynthesis, Plant, Cell Environ., 24(2), 253–259, doi:10.1046/j.1365-3040.2001.00668.x, 2001.

Chanson, M. and Millero, F. J.: Effect of filtration on the total alkalinity of open-ocean seawater, Limnol. Oceanogr. Methods, 5, 293–295, doi:10.4319/lom.2007.5.293, 2007.

Clarke, A.: Costs and consequences of evolutionary temperature adaptation, Trends Ecol. Evol., 18(11), 573–581, doi:10.1016/j.tree.2003.08.007, 2003.

Cohen, A. L. and Holcomb, M.: Why corals care about ocean acidification Uncovering the mechanism, Oceanography, 22(4), 118–127, doi:10.5670/oceanog.2009.102, 2009.

Cyronak, T., Santos, I. R. and Eyre, B. D.: Permeable coral reef sediment dissolution driven by elevated pCO2 and pore water advection, Geophys. Res. Lett., 40(18), 4876–4881, doi:10.1002/grl.50948, 2013.

Cyronak, T., Santos, I. R., McMahon, A. and Eyre, B. D.: Carbon cycling hysteresis in permeable carbonate sands over a diel cycle: Implications for ocean acidification, Limnol. Oceanogr., 58(1), 131–143, doi:10.4319/lo.2013.58.1.0131, 2013.

Cyronak, T. and Eyre, B. D.: The synergistic effects of ocean acidification and organic metabolism on calcium carbonate (CaCO3) dissolution in coral reef sediments, Mar. Chem., 183, 1–12, doi:10.1016/j.marchem.2016.05.001, 2016.

Díaz-ortega, G. and Hernández-Delgado, E. a: Unsustainable Land-Based Source Pollution in a Climate of Change: A Roadblock to the Conservation and Recovery of Elkhorn Coral Acropora palmata (Lamarck 1816), Nat. Resour., 5(10), 561–581, doi:10.4236/nr.2014.510050, 2014.

Dickson, A. G. and Millero, F. J.: A comparison of the equilibrium constants for the dissociation of carbonic acid in seawater media, Deep Sea Res. Part A. Oceanogr. Res. Pap., 34(10), 1733–1743, doi:10.1016/0198-0149(87)90021-5, 1987.

Dickson, A. G., Sabine, C. L. and Christian, J. R.: Guide to best practices for ocean CO2 measurements, North Pacific Marine Science Organization., 2007.

Ducklow, H. W. and Mitchell, R.: Composition of mucus released by coral reef coelenterates, Limnol. Oceanogr., 24(4), 706–714, doi:10.4319/lo.1979.24.4.0706, 1979.

508 Edinger, E. N., Jompa, J., Limmon, G. V, Widjatmoko, W. and Risk, M. J.: Reef degradation and coral
509 biodiversity in Indonesia: Effects of land-based pollution, destructive fishing practices and changes over
510 time, Mar. Pollut. Bull., 36(8), 617–630, doi:10.1016/S0025-326X(98)00047-2, 1998.

511 Eyre, B. D., Glud, R. N. and Patten, N.: Mass coral spawning: A natural large-scale nutrient addition
512 experiment, Limnol. Oceanogr., 53(3), 997–1013, doi:10.4319/lo.2008.53.3.0997, 2008.

513 Eyre, B. D., Ferguson, A. J. P., Webb, A., Maher, D. and Oakes, J. M.: Metabolism of different benthic habitats
514 and their contribution to the carbon budget of a shallow oligotrophic sub-tropical coastal system (southern
515 Moreton Bay, Australia), Biogeochemistry, 102(1), 87–110, doi:10.1007/s10533-010-9424-7, 2011.

516 Eyre, B. D., Santos, I. R. and Maher, D. T.: Seasonal, daily and diel N2 effluxes in permeable carbonate
517 sediments, Biogeosciences, 10(4), 2601–2615, doi:10.5194/bg-10-2601-2013, 2013

518 Eyre, B. D., Andersson, A. J. and Cyronak, T.: Benthic coral reef calcium carbonate dissolution in an acidifying
519 ocean, Nat. Clim. Chang., 4(11), 969–976, doi:10.1038/nclimate2380, 2014.

520 Eyre, B. D., Oakes, J. M. and Middelburg, J. J.: Fate of microphytobenthos nitrogen in subtropical subtidal
521 sediments: A 15N pulse-chase study, Limnol. Oceanogr., 61(6), 2108–2121, doi:10.1002/lno.10356, 2016.

522 Fabricius, K. E.: Effects of terrestrial runoff on the ecology of corals and coral reefs: Review and synthesis,
523 Mar. Pollut. Bull., 50(2), 125–146, doi:10.1016/j.marpolbul.2004.11.028, 2005.

524 Ferguson, A., Eyre, B. and Gay, J.: Organic matter and benthic metabolism in euphotic sediments along shallow
525 sub-tropical estuaries, northern New South Wales, Australia, Aquat. Microb. Ecol., 33(2), 137–154,
526 doi:10.3354/ame033137, 2003.

527 Ferrier-Pagès, C., Leclercq, N., Jaubert, J. and Pelegrí, S. P.: Enhancement of pico- and nanoplankton growth by
528 coral exudates, Aquat. Microb. Ecol., 21(2), 203–209, doi:10.3354/ame021203, 2000.

529 Frommlet, J. C., Sousa, M. L., Alves, A., Vieira, S. I., Suggett, D. J. and Serôdio, J.: Coral symbiotic algae
530 calcify ex hospite in partnership with bacteria., Proc. Natl. Acad. Sci. U. S. A., 112(19), 6158–63,
531 doi:10.1073/pnas.1420991112, 2015.

532 Furnas, M., Mitchell, A., Skuza, M. and Brodie, J.: In the other 90%: Phytoplankton responses to enhanced
533 nutrient availability in the Great Barrier Reef Lagoon, in Marine Pollution Bulletin, vol. 51, pp. 253–265.,
534 2005.

535 Glud, R. N., Eyre, B. D. and Patten, N.: Biogeochemical responses to mass coral spawning at the Great Barrier
536 Reef: Effects on respiration and primary production, Limnol. Oceanogr., 53(3), 1014–1024,
537 doi:10.4319/lo.2008.53.3.1014, 2008.

538 Grigg, R. W.: Coral reefs in an urban embayment in Hawaii: a complex case history controlled by natural and
539 anthropogenic stress, Coral Reefs, 14(4), 253–266, doi:10.1007/BF00334349, 1995.

540 Guillard, R. R. L.: Culture of Phytoplankton for Feeding Marine Invertebrates, in Culture of Marine Invertebrate
541 Animals, pp. 29–60, Springer US, Boston, MA., 1975.

542 Hancke, K. and Glud, R. N.: Temperature effects on respiration and photosynthesis in three diatom-dominated
543 benthic communities, Aquat. Microb. Ecol., 37(3), 265–281, doi:10.3354/ame037265, 2004.

544 Hancke, K., Sorrell, B. K., Chresten Lund-Hansen, L., Larsen, M., Hancke, T. and Glud, R. N.: Effects of
545 temperature and irradiance on a benthic microalgae community: A combined two-dimensional oxygen and
546 fluorescence imaging approach, Limnol. Oceanogr., 59(5), 1599–1611, doi:10.4319/lo.2014.59.5.1599,
547 2014.

548 Huettel, M. and Gust, G.: Solute release mechanisms from confined sediment cores in stirred benthic chambers
549 and flume flows, Mar. Ecol. Prog. Ser., 82, 187–197, doi:10.3354/meps082187, 1992.

550 IPCC Summary for policymakers. Climate Change 2013: The Physical Science Basis Contribution of Working
551 Group I to the Fifth Assessment Report of the Intergovernmental Panel on Climate Change. Cambridge
552 University Press, Cambridge, United Kingdom and New York, NY USA. 2013

553 Johnson, M. D. and Carpenter, R. C.: Ocean acidification and warming decrease calcification in the crustose
554 coralline alga Hydrolithon onkodes and increase susceptibility to grazing, J. Exp. Mar. Bio. Ecol., 434–435,
555 94–101, doi:10.1016/j.jembe.2012.08.005, 2012.

556 Koop, K., Booth, D., Broadbent, A., Brodie, J., Bucher, D., Capone, D., Coll, J., Dennison, W., Erdmann, M.,
557 Harrison, P., Hoegh-Guldberg, O., Hutchings, P., Jones, G. B., Larkum, A. W. D., O'Neil, J., Steven, A.,
558 Tentori, E., Ward, S., Williamson, J. and Yellowlees, D.: ENCORE: The effect of nutrient enrichment on
559 coral reefs. Synthesis of results and conclusions, Mar. Pollut. Bull., 42(2), 91–120, doi:10.1016/S0025-
560 326X(00)00181-8, 2001.

561 Lantz, C. A., Carpenter, R. C. and Edmunds, P. J.: Calcium carbonate (CaCO3) sediment dissolution under
562 elevated concentrations of carbon dioxide (CO2) and nitrate (NO3–), J. Exp. Mar. Bio. Ecol., 495(May), 48–
563 56, doi:10.1016/j.jembe.2017.05.014, 2017.

564 Lavigne, H. and Gattuso, J.P.:Package 'seacarb': seawater carbonate chemistry with R, v. 2.4. 8 (ed. R
565 Development Core Team). See http.cran.r-project.org/web/ packages/seacarb/index.html, 2013.

566 Lee, K. and Millero, F. J.: Thermodynamic studies of the carbonate system in seawater, Deep Sea Res. Part I
567 Oceanogr. Res. Pap., 42(11–12), 2035–2061, doi:10.1016/0967-0637(95)00077-1, 1995.

568 Levitus, S., Antonov, J. I., Boyer, T. P. and Stephens, C.: Warming of the World Ocean, Science (80-.).,
569 287(March), 2225–2229, doi:10.1126/science.287.5461.2225, 2000.

570 López-Urrutia, Á. and Morán, X. A. G.: Resource limitation of bacterial production distorts the temperature
571 dependence of oceanic carbon cycling, Ecology, 88(4), 817–822, doi:10.1890/06-1641, 2007.

572 Maher, D. T., Santos, I. R., Leuven, J. R. F. W., Oakes, J. M., Erler, D. V., Carvalho, M. C. and Eyre, B. D.:
573 Novel Use of Cavity Ring-down Spectroscopy to Investigate Aquatic Carbon Cycling from Microbial to
574 Ecosystem Scales, Environ. Sci. Technol., 47(22), 12938–12945, doi:10.1021/es4027776, 2013.

575 Mallela, J. and Perry, C. T.: Calcium carbonate budgets for two coral reefs affected by different terrestrial runoff
576 regimes, Rio Bueno, Jamaica, Coral Reefs, 26(1), 129–145, doi:10.1007/s00338-006-0169-7, 2007.

577 Mehrbach, C. and Carl: Measurement of the apparent dissociation constants of carbonic acid in seawater at
578 atmospheric pressure, 1973.

579 Middelburg, J. J., Soetaert, K. and Herman, P. M. J.: Empirical relationships for use in global diagenetic models,
580 Deep Sea Res. Part I Oceanogr. Res. Pap., 44(2), 327–344, doi:10.1016/S0967-0637(96)00101-X, 1997.

581 Moriarty, D. J. W., Pollard, P. C. and Hunt, W. G.: Temporal and spatial variation in bacterial production in the
582 water column over a coral reef, Mar. Biol., 85(3), 285–292, doi:10.1007/BF00393249, 1985.

583 Muehllehner, N., Langdon, C., Venti, A. and Kadko, D.: Dynamics of carbonate chemistry, production, and
584 calcification of the Florida Reef Tract (2009-2010): Evidence for seasonal dissolution, Global Biogeochem.
585 Cycles, 30(5), 661–688, doi:10.1002/2015GB005327, 2016.

586 Odum, H. T. and Odum, E. P.: Trophic Structure and Productivity of a Windward Coral Reef Community on
587 Eniwetok Atoll, Ecol. Monogr., 25(3), 291–320, doi:10.2307/1943285, 1955.

588 Orlando, J. L. and Yee, S. H.: Linking Terrigenous Sediment Delivery to Declines in Coral Reef Ecosystem
589 Services, Estuaries and Coasts, 40(2), 359–375, doi:10.1007/s12237-016-0167-0, 2017.

590 Pandolfi, J. M., Connolly, S. R., Marshall, D. J. and Cohen, A. L.: Projecting coral reef futures under global
591 warming and ocean acidification., Science (80-)., 333(6041), 418–422, doi:10.1126/science.1204794, 2011.

592 Rabalais, N. N., Turner, R. E., Díaz, R. J. and Justić, D.: Global change and eutrophication of coastal waters,
593 ICES J. Mar. Sci., 66(7), 1528–1537, doi:10.1093/icesjms/fsp047, 2009.

594 Rabouille, C., Mackenzie, F. T. and Ver, L. M.: Influence of the human perturbation on carbon, nitrogen, and
595 oxygen biogeochemical cycles in the global coastal ocean, Geochim. Cosmochim. Acta, 65(21), 3615–3641,
596 doi:10.1016/S0016-7037(01)00760-8, 2001.

597 Robinson, C.: Plankton gross production and respiration in the shallow water hydrothermal systems of Miles,
598 Aegean Sea, J. Plankton Res., 22(5), 887–906, doi:10.1093/plankt/22.5.887, 2000.

599 Roelfsema, R. T. C. M. and Roelfsema, R. T. C. M.: Spatial distribution of benthic microalgae on coral reefs
600 determined by remote sensing, Coral Reefs, 21(3), 264–274, doi:10.1007/s00338-002-0242-9, 2002.

601 Salmond, J, Loder, J, Roelfsema, C, Host, R, Passenger, J.: 2015 Heron Reef Health Report, Brisbane., 2015.

602 Shaw, E. C., Carpenter, R. C., Lantz, C. A. and Edmunds, P. J.: Intraspecific variability in the response to ocean
603 warming and acidification in the scleractinian coral Acropora pulchra, Mar. Biol., 163(10), 210,
604 doi:10.1007/s00227-016-2986-8, 2016.

605 SPSS Inc. IBM Corp. IBM SPSS Statistics for Windows, Version 22.0. Armonk, NY: IBM Corp, 2013.

606 Tait, L. W. and Schiel, D. R.: Impacts of Temperature on Primary Productivity and Respiration in Naturally
607 Structured Macroalgal Assemblages, edited by T. Crowe, PLoS One, 8(9), e74413,
608 doi:10.1371/journal.pone.0074413, 2013.

609 Trnovsky, D., Stoltenberg, L., Cyronak, T. and Eyre, B.D.: Antagonistic Effects of Ocean Acidification and
610 Rising Sea Surface Temperature on the Dissolution of Coral Reef Carbonate Sediments. Front in Mar Sci 3,
611 211, doi:10.3389/fmars.2016.00211, 2016.

612 Weston, N. B. and Joye, S. B.: Temperature-driven decoupling of key phases of organic matter degradation in
613 marine sediments, Proc. Natl. Acad. Sci. U. S. A., 102(47), 17036–17040, doi:10.1073/pnas.0508798102,
614 2005.

615 Wiencke, C., Rahmel, J., Karsten, U., Weykam, G. and Kirst, G. O.: Photosynthesis of marine macroalgae from
616 Antarctica: Light and temperature requirements, Bot Act, 106(1), 78–87, doi:10.1111/j.1438-
617 8677.1993.tb00341.x, 1993.

618 Wild, C., Huettel, M., Klueter, A., Kremb, S. G., Rasheed, M. Y. M. and Jørgensen, B. B.: Coral mucus
619 functions as an energy carrier and particle trap in the reef ecosystem., Nature, 428(6978), 66–70,
620 doi:10.1038/nature02344, 2004.

621 Wild, C., Rasheed, M., Werner, U., Franke, U., Johnstone, R. and Huettel, M.: Degradation and mineralization
622 of coral mucus in reef environments, Mar. Ecol. Prog. Ser., 267, 159–171, doi:10.3354/meps267159, 2004.

623 Wild, C., Rasheed, M., Jantzen, C., Cook, P., Struck, U., Huettel, M. and Boetius, A.: Benthic metabolism and
624 degradation of natural particulate organic matter in carbonate and silicate reef sands of the northern Red Sea,
625 Mar. Ecol. Prog. Ser., 298, 69–78, doi:10.3354/meps298069, 2005.

626 Wilkinson, C. R.: Microbial ecology on a coral reef, Search, 18, 31–33, 1987.Woodwell, G. M., Mackenzie, F.
627 T., Houghton, R. A., Apps, M., Gorham, E. and Davidson, E.: Biotic feedbacks in the warming of the earth,
628 Clim. Change, 40(3/4), 495–518, doi:10.1023/A:1005345429236, 1998.

629 Yamano, H., Miyajima, T. and Koike, I.: Importance of foraminifera for the formation and maintenance of a
630 coral sand cay: Green Island, Australia, Coral Reefs, 19(1), 51–58, doi:10.1007/s003380050226, 2000.

631 Yeakel, K. L., Andersson, A. J., Bates, N. R., Noyes, T. J., Collins, A., and Garley, R.: Shifts in coral reef
632 biogeochemistry and resulting acidification linked to offshore productivity. Proc. of the Nat. Acad. of Sci.,
633 112(47), 14512–14517. doi:10.1073/pnas.1507021112, 2015.

634 Yvon-Durocher, G., Jones, J. I., Trimmer, M., Woodward, G. and Montoya, J. M.: Warming alters the metabolic
635 balance of ecosystems, Philos. Trans. R. Soc. B Biol. Sci., 365(1549), 2117–2126,
636 doi:10.1098/rstb.2010.0038, 2010.

637 **Tables**

Table 1: Concentrations of carbon (µmol C L^{-1}) and nitrogen (µmol N L^{-1}) and measured temperature (ºC) in the control and treatment chambers. Values correspond to the mean ± SD.

Treatment	Carbon (µmol C L^{-1})	Nitrogen (µmol N L^{-1})	Temperature (ºC)
C	0.63 ± 0.13	0.12 ± 0.08	28.2 ± 1.1
T	0.63 ± 0.13	0.12 ± 0.08	30.6 ± 1.0
PD	21.7 ± 1.0	2.3 ± 0.8	28.4 ± 1.0
T + PD	21.7 ± 1.0	2.3 ± 0.8	30.5 ± 0.9
CM	24.2 ± 1.1	1.5 ± 0.4	28.3 ± 0.8
T + CM	24.2 ± 1.1	1.5 ± 0.4	30.7 ± 1.1

Table 2: The equations used in this study to calculate rates of sediment metabolism based on measured fluxes in dissolved oxygen (DO) and total alkalinity (A_T) (Eyre et al. (2011).

Metabolic Rate	Definition
Respiration (R)	Dark DO Flux x -1
Net Primary Production (NPP)	Light DO Flux
Gross Primary Production (GPP)	NPP + R
GPP/R	GPP x 12 (daylight hours)/ R x 24 (total hours)
Net Calcification (G_{net})	A_T Flux x 0.5; positive values represent net calcification and negative rates represent net dissolution

Table 3: Calculated respiration (R: mmol O_2 m^{-2} hr^{-1}), net primary productivity (NPP: mmol O_2 m^{-2} hr^{-1}), gross primary productivity (GPP: mmol O_2 m^{-2} hr^{-1}), the ratio of GPP/R, and net calcification (G_{net}: mmol $CaCO_3$ m^{-2} hr^{-1}) in the control and treatment chambers. Values correspond to the mean ± SD.

Treatment	R (mmol O_2 m^{-2} hr^{-1})	NPP (mmol O_2 m^{-2} hr^{-1})	GPP (mmol O_2 m^{-2} hr^{-1})	GPP/R	Day G_{net} (mmol $CaCO_3$ m^{-2} hr^{-1})	Night G_{net} (mmol $CaCO_3$ m^{-2} hr^{-1})	Diel G_{net} (mmol $CaCO_3$ m^{-2} hr^{-1})
C	- 1.3 ± 0.5	1.9 ± 0.3	3.2 ± 0.4	1.31 ± 0.1	1.3 ± 0.2	- 0.9 ± 0.2	0.2 ± 0.2
T	- 3.5 ± 0.4	2.9 ± 0.4	6.4 ± 0.5	0.91 ± 0.1	1.7 ± 0.2	- 1.9 ± 0.2	- 0.2 ± 0.1
PD	- 2.6 ± 0.5	5.3 ± 0.5	7.9 ± 0.4	1.54 ± 0.1	2.8 ± 0.3	- 1.5 ± 0.2	0.6 ± 0.2
T + PD	- 3.1 ± 0.5	4.7 ± 0.5	7.8 ± 0.5	1.27 ± 0.1	2.6 ± 0.3	- 1.9 ± 0.2	0.3 ± 0.1
CM	- 2.0 ± 0.4	4.4 ± 0.4	6.4 ± 0.7	1.61 ± 0.2	2.4 ± 0.3	- 1.3 ± 0.2	0.5 ± 0.2
T + CM	- 2.9 ± 0.4	4.6 ± 0.5	7.4 ± 0.5	1.25 ± 0.1	2.3 ± 0.4	- 1.8 ± 0.3	0.2 ± 0.2

Table 4: A comparison of studies which employed the same methodology (advective chamber incubations) under a similar advection rate (~ 43 L m^{-2} d^{-1}) and calculated gross primary productivity (GPP: mmol O_2 m^{-2} hr^{-1}) respiration (R: mmol O_2 m^{-2} hr^{-1}), the ratio of GPP/R, and net calcification (G_{net}: mmol $CaCO_3$ m^{-2} hr^{-1}) under ambient conditions. This study, data from Cyronak et al. (2013a, 2013b, and 2016), and Trnovsky et al. (2016) were collected in-situ at Heron Island, Australia while data from Lantz et al. (2017) were collected ex-situ in Moorea. French Polynesia.

Study	R (mmol O_2 m^{-2} hr^{-1})	GPP (mmol O_2 m^{-2} hr^{-1})	GPP/R	G_{net} (mmol $CaCO_3$ m^{-2} hr^{-1})
This Study	- 1.3 ± 0.5	3.2 ± 0.4	1.31 ± 0.1	0.2 ± 0.2
Cyronak et al., 2013a	N/A	N/A	N/A	0.1 ± 0.1
Cyronak et al., 2013b	N/A	N/A	N/A	0.2 ± 0.1
Cyronak et al., 2016	- 2.5 ± 0.1	6.3 ± 0.2	1.27 ± 0.1	0.4 ± 0.2
Trnovsky et al., 2016	- 2.1 ± 0.6	5.1 ± 0.8	1.29 ± 0.2	0.6 ± 0.3
Lantz et al., 2017	N/A	N/A	N/A	0.1 ± 0.1

638 **Figures**

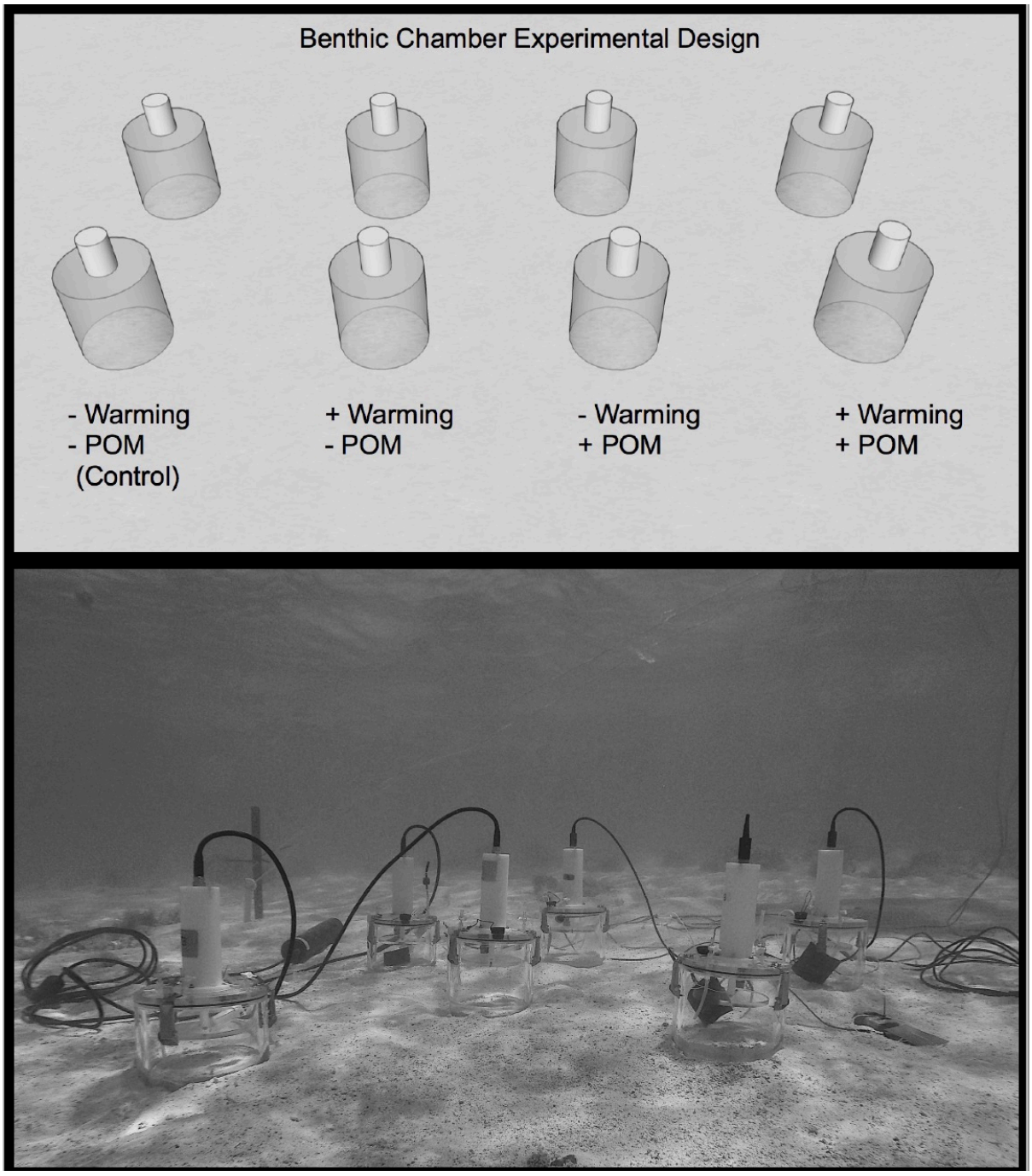

639

640 **Figure 1:** Layout of the experimental design using benthic chambers. Eight chambers were used in total, which
641 provided two replicates per treatment. Chambers are organized by the presence (+) and absence (-) of the
642 warming (+2.4 ºC) and organic matter (OM) (phytodetritus or coral mucus) treatments.

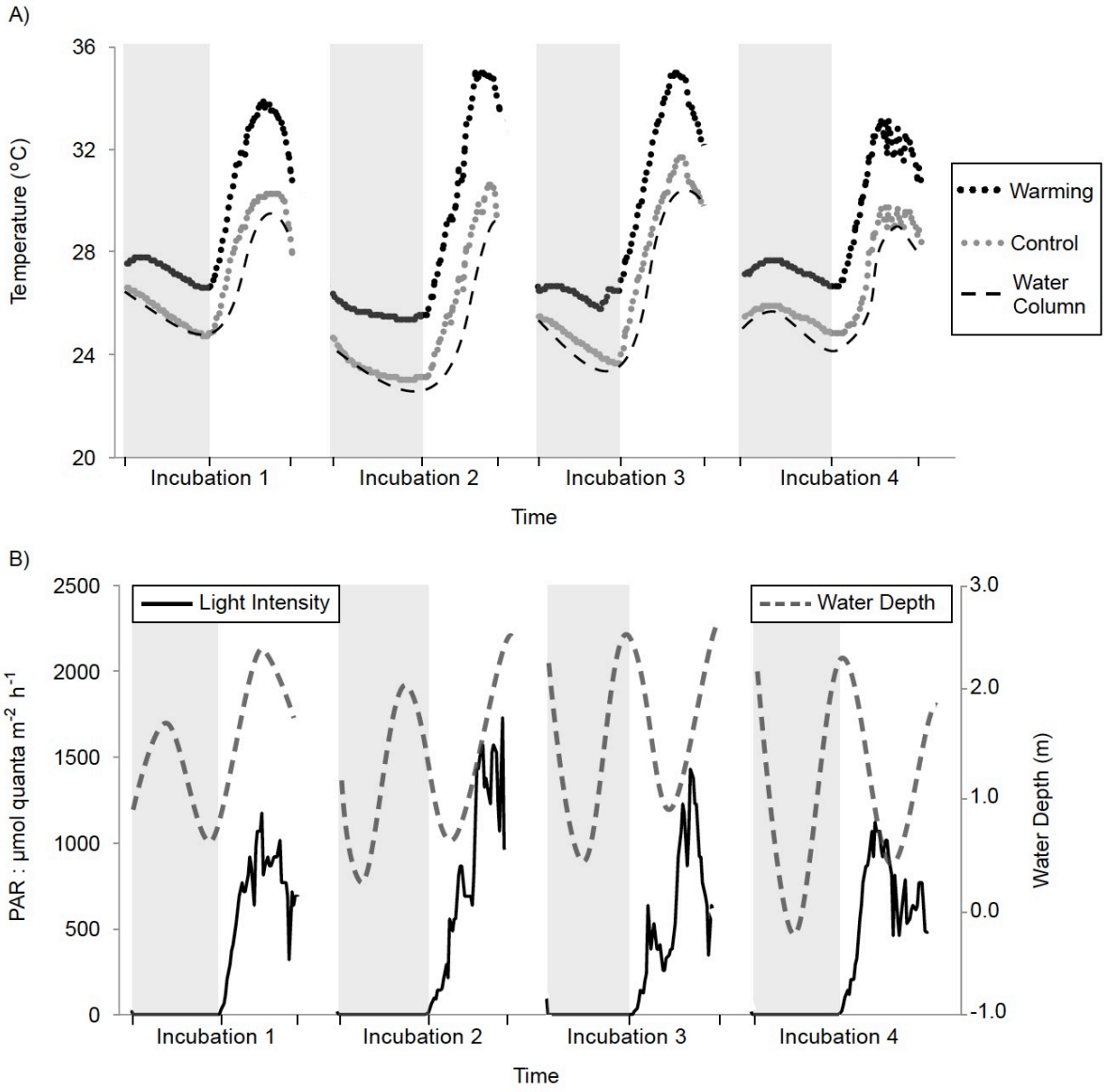

643

644 **Figure 2:** Water column parameters measured during the four incubations, each starting at sunset (18:00) and
645 ending at the following day's dusk (16:00). Data are presented from the first phase (Incubation 1 and 2) where
646 phytodetritus was used as an organic matter (OM) treatment, and from the second phase (Incubation 3 and 4),
647 where coral mucus was used as an OM treatment. Shaded grey bars represent nighttime. A) Mean temperature
648 (ºC) measured by Hobo temperature recorders that logged temperature at fifteen-minute intervals during each
649 incubation period. Data are pooled together as the mean from control (grey dots) and warming (black dots)
650 treatments (n = 4 per incubation). Mean water column temperature (n = 1 per incubation) shown as a black
651 dash. B) Measured light intensity (µmol quanta m^{-2} s^{-1}) in the water column (black line) and water height (m)
652 during each incubation period (grey dash).

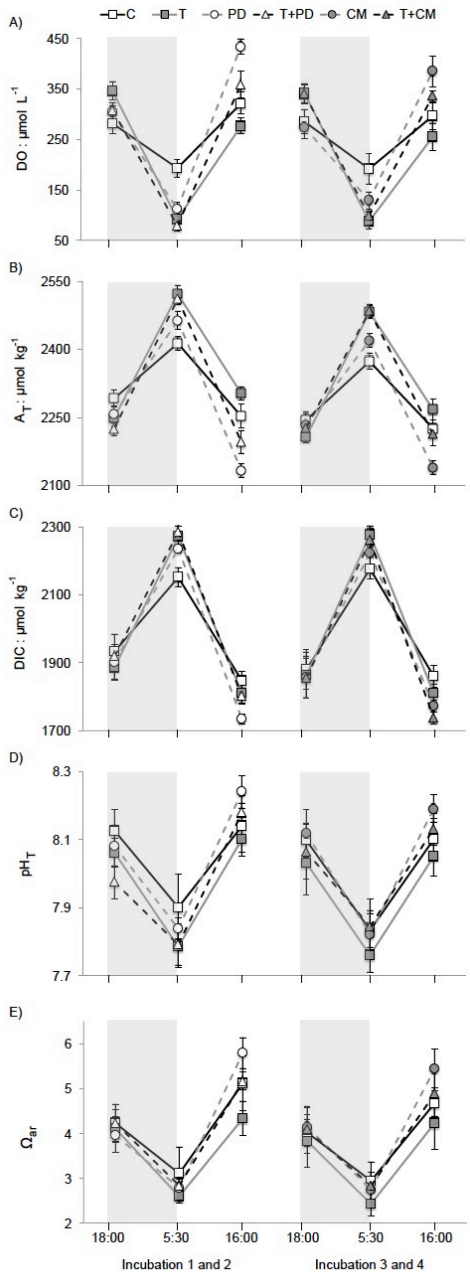

653

654 **Figure 3:** Water chemistry (mean ± SD) measured and calculated during the four incubations. Control (C),
655 warming (T), phytodetritus (PD), coral mucus (CM), and combination (T + PD, T + CM) treatments are
656 averaged over the two incubations (and replicate chambers therein) in which each respective OM treatment was
657 used (n = 4). Shaded grey bars represent the dark and time of sampling is labelled on the x-axis. A) Measured
658 fluxes in dissolved oxygen (DO: µmol L^{-1}). B) Measured fluxes in total alkalinity (A_T: µmol kg^{-1}). C) Measured
659 fluxes in dissolved inorganic carbon (DIC: µmol kg^{-1}). D) Calculated changes in pH (total scale: pH_T). E)
660 Calculated fluxes in aragonite saturation state (Ω_{ar}).

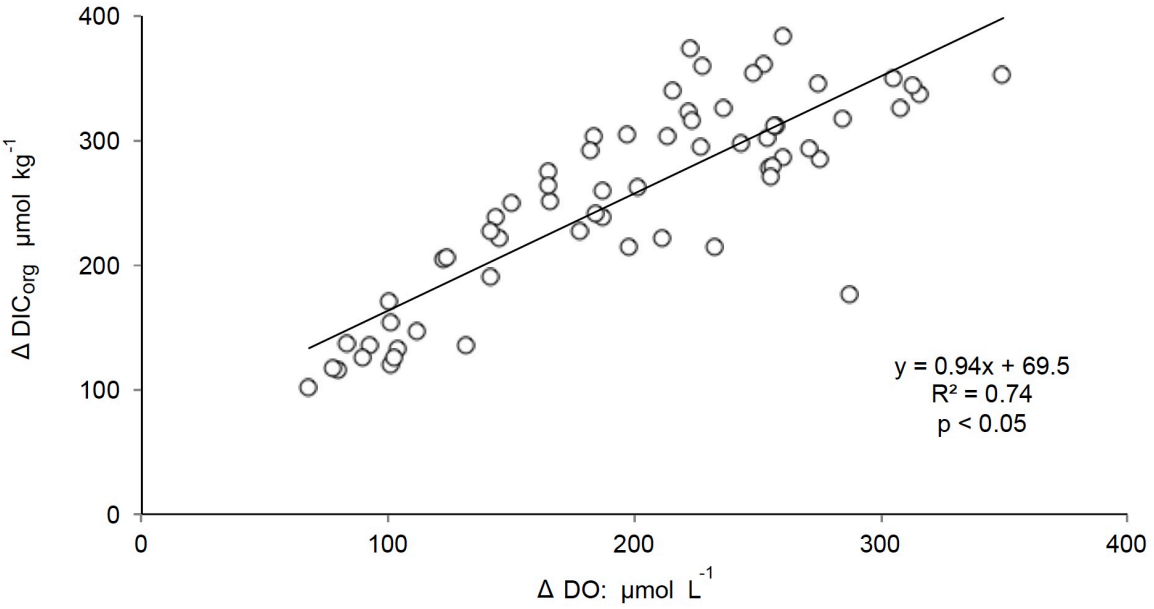

661

662 **Figure 4:** A linear correlation between calculated changes in dissolved inorganic carbon (ΔDIC_{org}: µmol kg^{-1}) as
663 a function of measured changes in dissolved oxygen (ΔDO: µmol L^{-1}) over each 12-hour sampling period from
664 all chambers and incubations. To examine the variation in DIC due solely to photosynthesis and respiration
665 (DIC_{org}), changes in DIC were corrected for calcium carbonate precipitation/dissolution using the measured
666 changes in total alkalinity (A_T) (0.5 moles CO_2: 1 mole A_T).

667

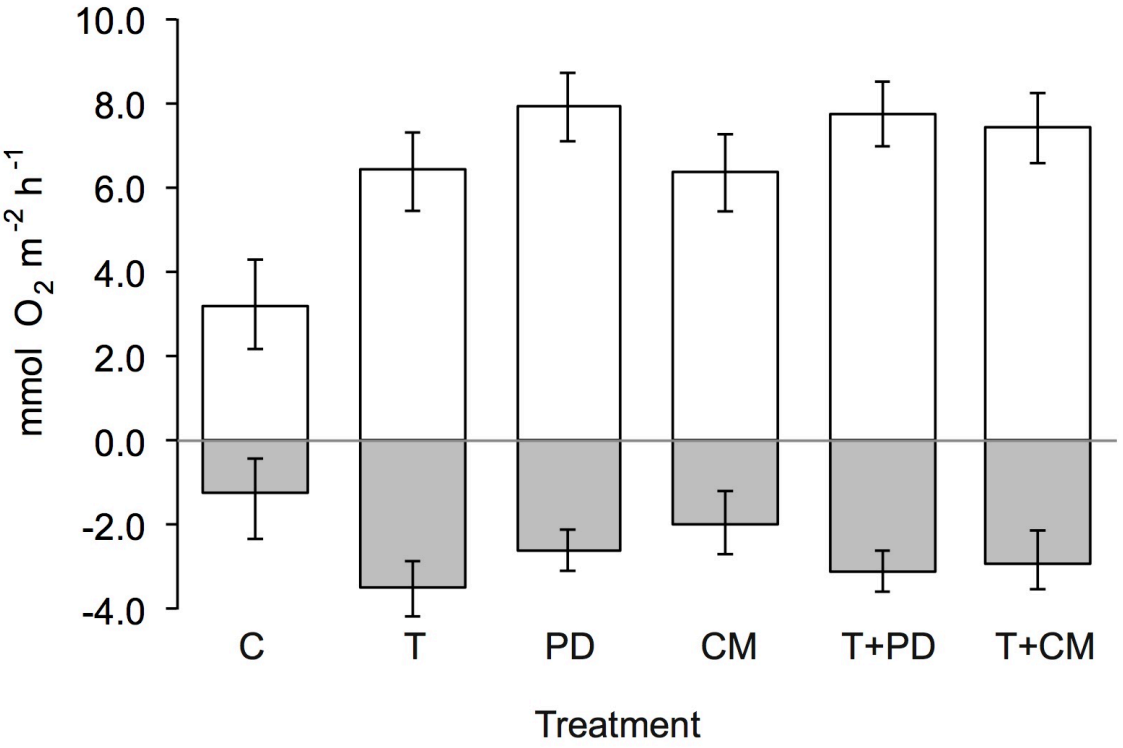

668

669 **Figure 5:** Mean sediment gross primary production (GPP: mmol O_2 m^{-2} h^{-1}) and respiration (R: mmol O_2 m^{-2} h^{-1}) in response to warming (+2.4 ºC) and each OM treatment (phytodetritus and coral mucus). Control (C) (n = 9) and warming (T) (n = 7) treatments are averaged over all four incubations and the replicate chambers therein. Phytodetritus (PD), coral mucus (CM), and combination (T + PD, T + CM) treatments are averaged over the two incubations (and replicate chambers therein) in which each respective OM treatment was used (n = 4). Average measured rates ± SD are represented in white for GPP (positive) and grey for R (negative).

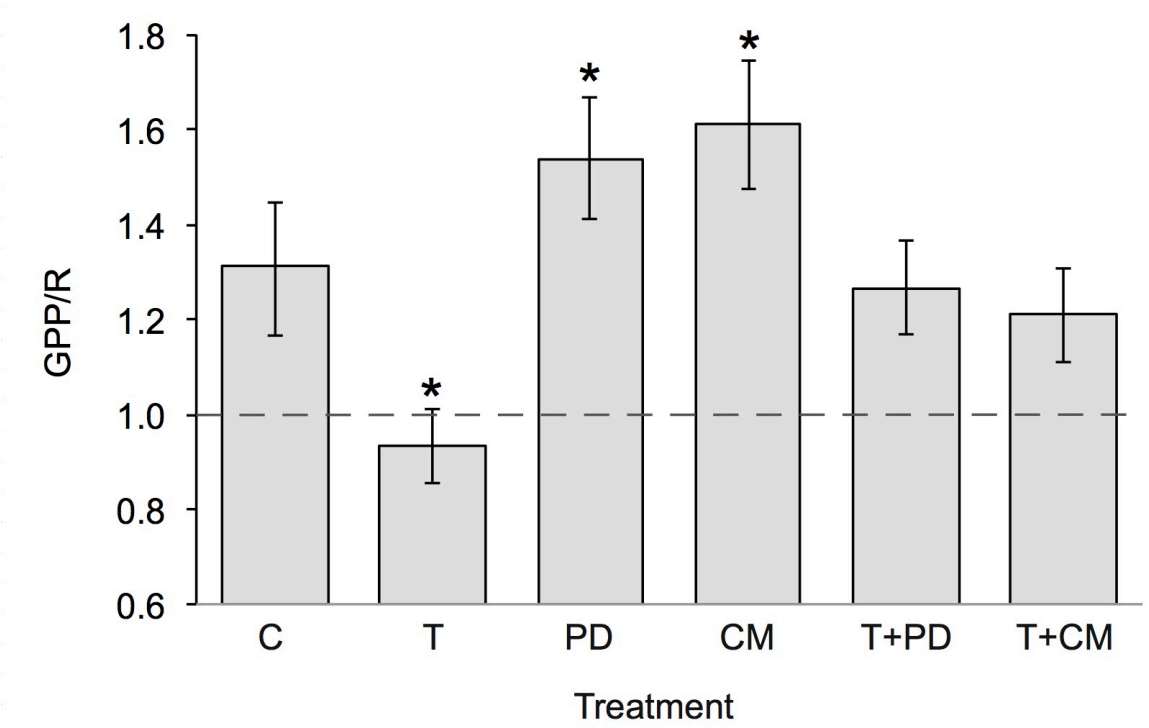

675

676 **Figure 6:** Sediment gross primary production (12 hour) to respiration (24 hour) ratios (GPP/R) in response to
677 warming (+2.4 ºC) and each OM treatment (phytodetritus and coral mucus). Control (C) (n = 9) and warming
678 (T) (n = 7) treatments are averaged over all four incubations and the replicate chambers therein, while
679 phytodetritus (PD), coral mucus (CM), and combination (T + PD, T + CM) treatments are averaged over the two
680 incubations (and replicate chambers therein) in which each respective OM treatment was used (n = 4). Dashed
681 grey line represents the divide between net heterotrophy and net autotrophy (GPP/R = 1) while the * indicates if
682 the presented value is significantly different the control.

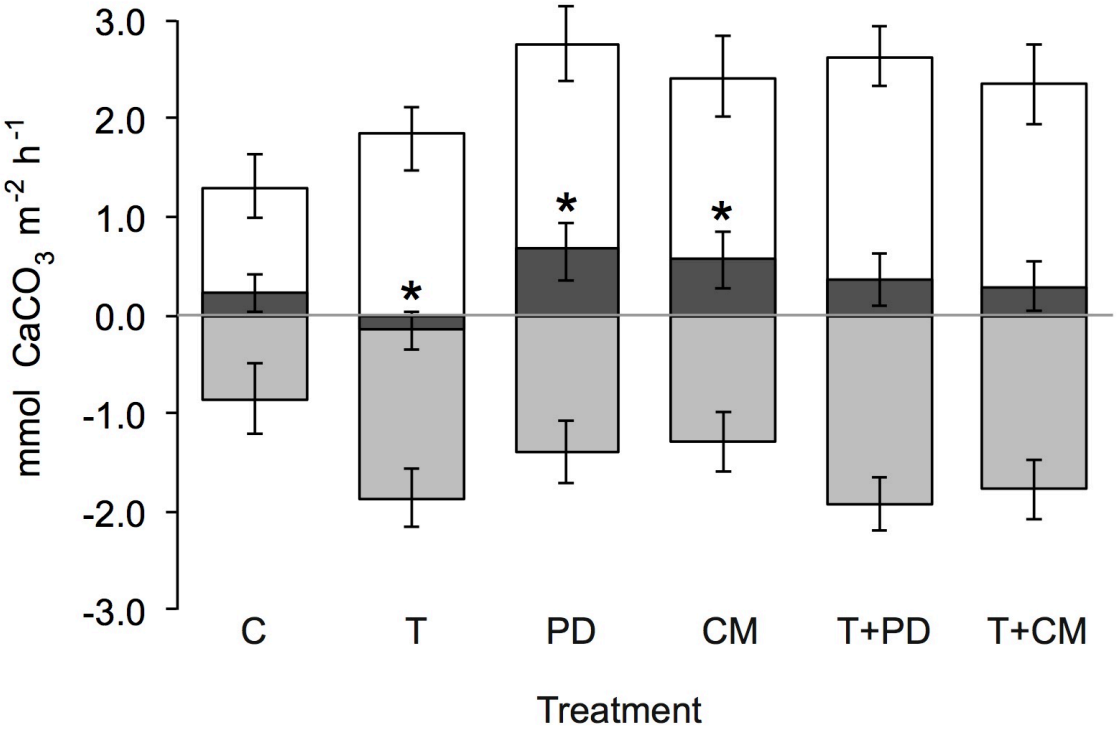

683

684 **Figure 7:** Mean sediment net calcification (G_{net}: mmol $CaCO_3$ m^{-2} h^{-1}) in response to warming (+2.4 ºC) and
685 each OM treatment (phytodetritus and coral mucus). Control (C) (n = 9) and warming (T) (n = 7) treatments are
686 averaged over all four incubations and the replicate chambers therein, while phytodetritus (PD), coral mucus
687 (CM), and combination (T + PD, T + CM) treatments are averaged over the two incubations (and replicate
688 chambers therein) in which each respective OM treatment was used (n = 4). Average measured rates ± SD are
689 represented in white for light G_{net} (positive) and grey for dark G_{net} (negative). Black bars represent the 24-hour
690 diel G_{net} averaged from light and dark measurements and the * next to these bars indicates if the value is
691 significantly different from the control.

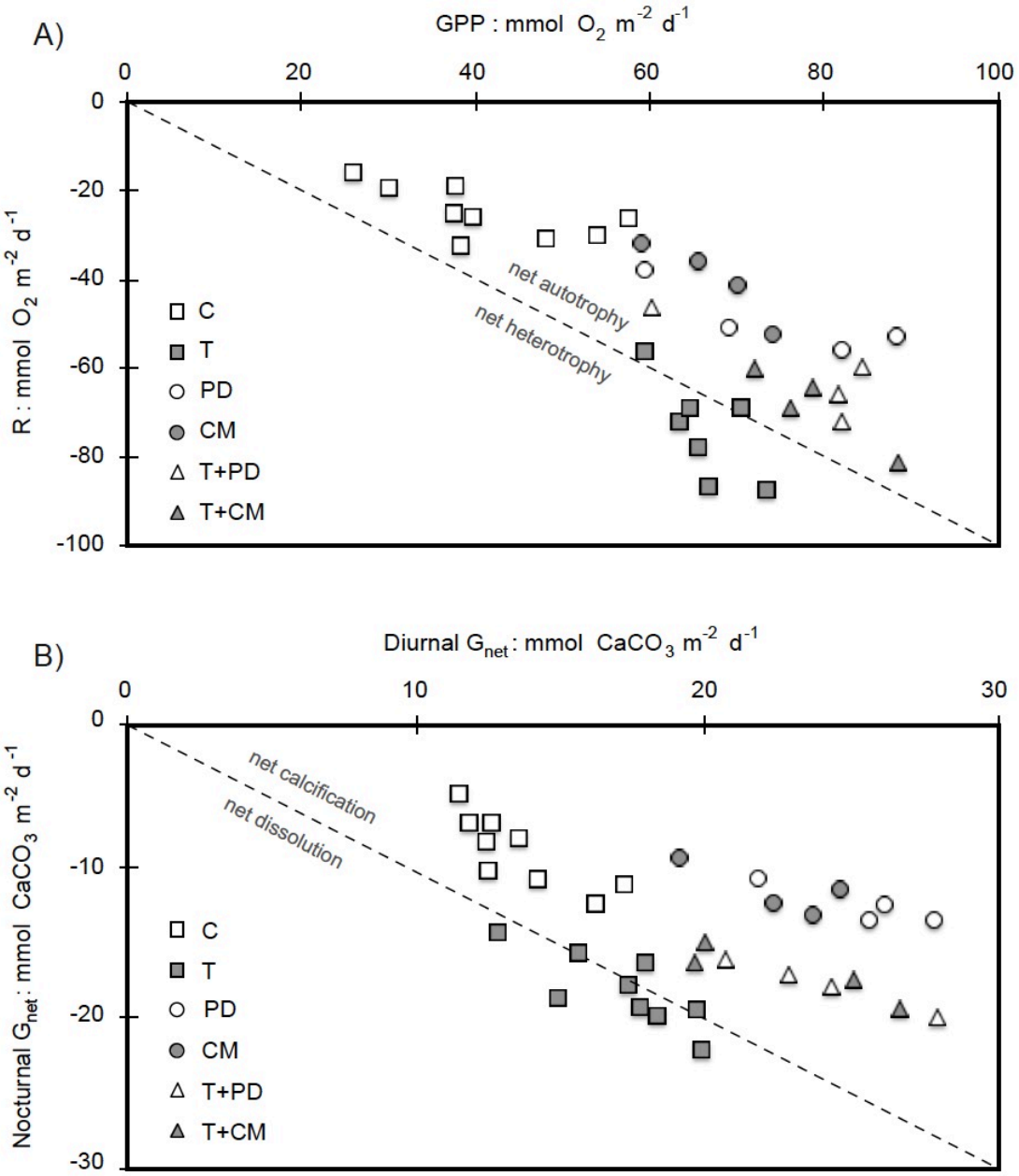

692

693 **Figure 8:** Measured metabolic rates from the control (C) (n = 9) and warming (T) (n = 7) treatments are
694 displayed from all four incubations and the replicate chambers therein. Phytodetritus (PD), coral mucus (CM),
695 and combination (T + PD, T + CM) treatments are displayed from the two incubations (and replicate chambers
696 therein) where each respective OM treatment was used (n = 4). A) Respiration (R: mmol O_2 m^{-2} d^{-1}) plotted as a
697 function of gross primary production (GPP: mmol O_2 m^{-2} d^{-1}). Dashed line represents the divide between net
698 heterotrophy and net autotrophy (GPP/R = 1). B) Dark dissolution (Dark G: mmol $CaCO_3$ m^{-2} d^{-1}) plotted as a
699 function of daytime calcification (Diurnal G: mmol $CaCO_3$ m^{-2} d^{-1}). Dashed line represents the divide between
700 net calcification and net dissolution (G_{net} = 0).